BIFURCATION ANALYSIS OF A POWER-FACTOR-CORRECTION BOOST CONVERTER: UNCOVERING FAST-SCALE INSTABILITY

Chi K. Tse and Octavian Dranga

Dept. of Electronic & Information Engineering
The Hong Kong Polytechnic University
Hung Hom, Kowloon, Hong Kong

Herbert H. C. Iu

Dept. of Electrical & Electronic Engineering
University of Western Australia
Perth, Australia

ABSTRACT

Bifurcation analysis is performed to a power-factor-correction (PFC) boost converter to examine the fast-scale instability problem. Computer simulations and analysis reveal the possibility of period-doubling for some intervals within the line cycle. The results allow convenient prediction of stability boundaries. Analytical equations and design curves are given to facilitate the selection of parameter values to guarantee stable operation.

Index Terms— Bifurcation analysis, dc/dc converters, power factor correction.

1. INTRODUCTION

The purpose of this paper is to examine the stability problem of a common power-factor-correction (PFC) boost converter from a bifurcation perspective. The control takes on a standard peak current-programming of the inductor (input) current, with the reference template closely following the input voltage waveshape, i.e., a rectified sine wave. The situation is similar to applying a slowly time-varying ramp compensation to a current-programmed boost converter. In this paper, we study the onset of period-doubling (fast-scale) instability in this converter. Specifically, we show that, with improper choice of parameters, the PFC boost converter can suffer from fast-scale instability for some intervals of time during the line cycle. Computer simulations are presented. Analytical equations and design curves are also given to facilitate the design of this type of converter to avoid fast-scale instability for all times.

2. SYSTEM DESCRIPTION

The circuit schematic of the PFC boost converter under study is shown in Fig. 1 [1]. Essentially, it is a typical current-programmed boost converter, with the inductor current i_L chosen as the programming variable and the programming template i_{ref} being the input voltage waveform [2, 3]. Obviously the average input current is programmed to track the input voltage, and hence the power factor is kept near unity. In addition, a feedback loop comprising a first-order filter and a PI controller serves to control the output voltage v_o (V_{ref} is the reference steady-state output voltage) by adjusting the amplitude of i_{ref}.

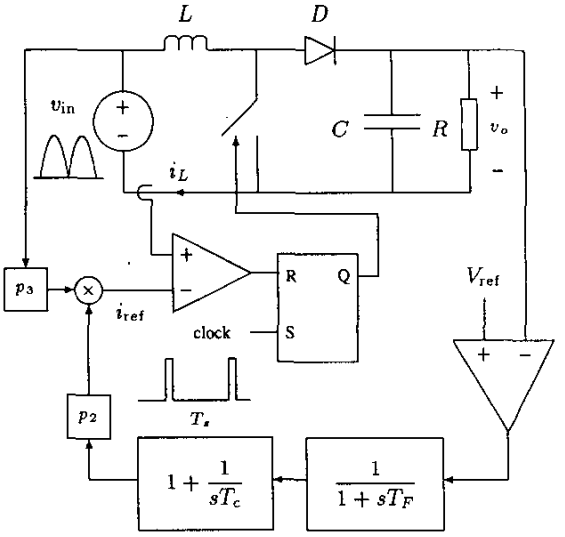

Fig. 1: Schematic of the PFC boost converter showing direct programming of the input current i_L. The reference current i_{ref} is a rectified sine wave whose amplitude is adjusted by the feedback loop to match the power level.

3. BIFURCATION BEHAVIOUR BY COMPUTER SIMULATIONS

Bifurcation and chaotic behaviour have been found previously in current-programmed converters under a dc input condition [4]–[6]. However, for the case of PFC applications, very little has been reported regarding the nonlinear behaviour of the circuit. In this section we begin with a series of computer simulations to identify possible bifurcation phenomena. The circuit component values used in the study

0-7803-7761-3/03/$17.00 ©2003 IEEE

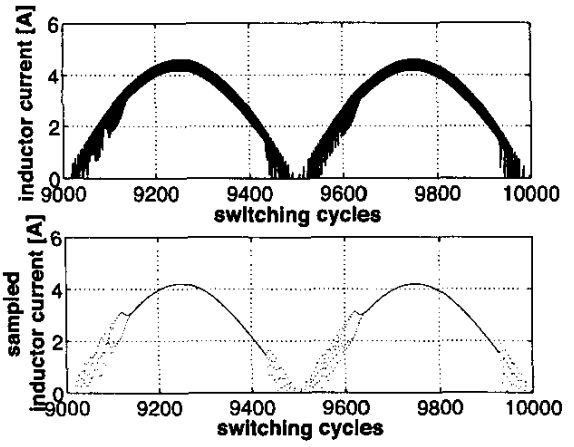

Fig. 2: Simulated inductor current time-domain waveform (upper) and the same waveform sampled at the switching frequency (lower) for $V_{\text{ref}} = 220$ V, i.e., $r_v = V_{\text{ref}}/\hat{V}_{\text{in}} = \sqrt{2}$.

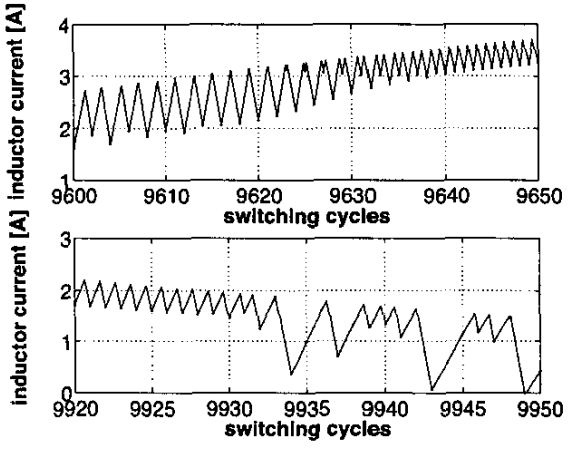

Fig. 3: Close-up view of Fig. 2 near the critical points.

are as follows: input voltage $v_{\text{in}} = 110$ V rms at 50 Hz; reference output voltage $V_{\text{ref}} = 220$–400 V; switching period $T_s = 20\ \mu$s; inductance $L = 2$ mH; capacitance $C = 470\ \mu$F; load resistance $R = 135\ \Omega$; filter time constant $T_F = 4$ ms; PI controller time constant $T_c = 1/70$ s; feedback gain $p_2 = 1/60$; gain $p_3 = 0.08$.

Figure 2 shows the simulated inductor current waveform $i_L(t)$ for $V_{\text{ref}} = 220$ V. Period-doubling bifurcation (or fast-scale instability) can be observed during the half line cycle, as shown in Fig. 2 (upper). In order to see the period-doubling more clearly and the *critical points* where the bifurcation starts, the waveform is sampled at a rate equal to the switching frequency, as shown in Fig. 2 (lower), where the two *critical points* can be clearly located. Between these two points the sampled values of the inductor current follow accurately the sinusoidal shape of the reference current i_{ref}.

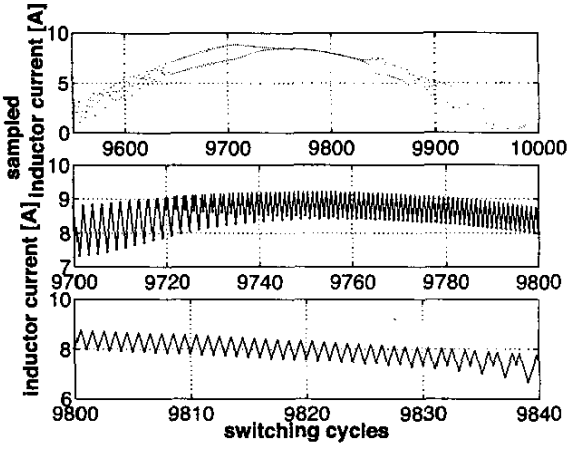

Fig. 4: Simulated sampled inductor current (upper) and close-up views of simulated waveform near critical points (middle and lower) when one critical phase angle (θ_{c1}) reaches 90° for $V_{\text{ref}} = 220\sqrt{2}$ V, i.e., $r_v = V_{\text{ref}}/\hat{V}_{\text{in}} = 2$

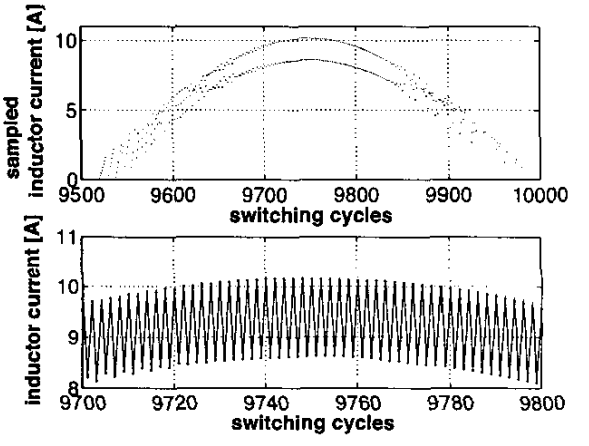

Fig. 5: Simulated sampled inductor current (upper) and close-up view of the inductor current waveform (lower) in full-bifurcation operation at $V_{\text{ref}} = 275\sqrt{2}$ V, i.e., $r_v = V_{\text{ref}}/\hat{V}_{\text{in}} = 2.5$.

We also note from Fig. 2 that the behaviour is chaotic near the zero crossing of the line cycle.[1] A close-up view of the waveform around the critical points is shown in Fig. 3. In the following we denote the critical points in terms of the phase angle $\theta = \omega_m t$, where ω_m is the line angular frequency. For brevity we define r_v as

$$r_v = V_{\text{ref}}/\hat{V}_{\text{in}} \tag{1}$$

where $\hat{V}_{\text{in}}$ is the amplitude of the input voltage, i.e.,

$$v_{\text{in}}(\theta) = \hat{V}_{\text{in}} \left|\sin\theta\right|. \tag{2}$$

[1] Our main concern here is the location of critical points since the occurrence of the first period-doubling bifurcation at the critical points is considered undesirable from the engineering viewpoint.

Here, we observe that the converter fails to maintain the expected "stable" operation in intervals corresponding to $\theta < \theta_{c1}$ and $\theta > \theta_{c2}$.

The fast-scale instability characterized by the presence of a critical point in each quarter of the line cycle persists until the left-hand side critical phase angle θ_{c1} reaches its maximum, i.e., 90^o, corresponding to the peak current value. The result of increasing further r_v beyond this point is shown in Fig. 4. Also, when θ_{c1} becomes greater than 90^o, the whole first quarter cycle has been fast-scale unstable, i.e., turned into period-doubling and possibly chaos in some intervals. Finally, fast-scale instability for the entire line cycle can be observed by increasing r_v further, as shown in Fig. 5.

4. ANALYSIS OF FAST-SCALE INSTABILITY

In this section we confirm the above simulation findings by analyzing the bifurcation behaviour of the PFC boost converter. By inspecting the iterative function that describes the inductor current dynamics, the critical duty ratio at which the first period-doubling occurs, D_c, can be obtained [7]:

$$D_c = \frac{M_c + 0.5}{M_c + 1} \tag{3}$$

where M_c is given by

$$M_c = \frac{m_c L}{v_{\text{in}}} \tag{4}$$

and m_c is the compensation slope defined in Fig. 6. Note that by applying a positive compensating ramp to the reference current (i.e., $M_c > 0$), the critical duty ratio given by (3) exceeds the value of 0.5 corresponding to the absence of the compensating ramp. Hence, it is obvious that compensation effectively provides more margin for the system to operate without fast-scale instability (period-doubling).

For the PFC boost converter under study, since the reference current i_{ref} follows the input voltage v_{in}, its waveform is a rectified sine wave whose frequency is much lower than the switching frequency (1000 times less in this case). Hence, the situation is analogous to the case of applying a time-varying ramp compensation to a peak current-programmed boost converter, as shown in Fig. 7.

Our aim here is to find the critical phase angle θ_c. From (2) to (4), and using $\frac{V_{\text{ref}}}{v_{\text{in}}} = \frac{1}{1-D}$ and $m_c = -di_{\text{ref}}/dt$, where D is the duty ratio, we get

$$|\sin\theta_c| = \frac{V_{\text{ref}} + 2L\frac{di_{\text{ref}}}{dt}}{2\hat{V}_{\text{in}}}. \tag{5}$$

If the power factor approaches one, the reference current is $i_{\text{ref}} \approx \hat{I}_{\text{L}} |\sin\theta|$, where $\hat{I}_{\text{L}}$ is the peak inductor reference current. Since the waveform is repeated for every $[k\pi, (k+1)\pi]$ interval, for all integers k, the analysis is restricted to

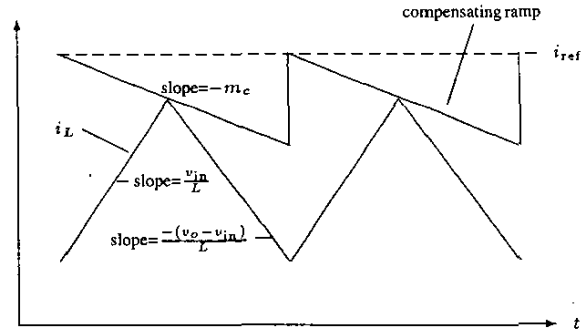

Fig. 6: Peak current-programming with ramp compensation.

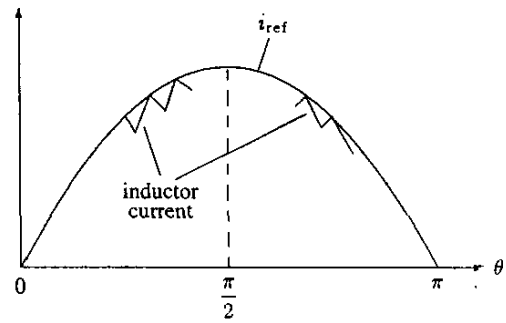

Fig. 7: Programming of input current waveform in PFC boost converter. For $0 \le \theta < \pi/2$, an effective negative ramp compensation is applied (i.e., $M_c < 0$), whereas for $\pi/2 < \theta \le \pi$, an effective positive ramp compensation is applied (i.e., $M_c > 0$).

the range $0 \le \theta \le \pi$. Therefore, $\frac{di_{\text{ref}}}{dt} \approx \omega_m \hat{I}_{\text{L}} \cos\theta$, and hence from (5), we obtain

$$\theta_c = 2\arctan\left(\frac{2\hat{V}_{\text{in}} \pm \sqrt{4\hat{V}_{\text{in}}^2 - V_{\text{ref}}^2 + 4\omega_m^2 \hat{I}_L^2 L^2}}{V_{\text{ref}} - 2\omega_m \hat{I}_L L}\right) \tag{6}$$

Moreover, incorporating the power equality, i.e., $\hat{V}_{\text{in}}\hat{I}_{\text{L}} = 2V_{\text{ref}}^2/R$ (assuming 100% efficiency), the critical phase angle given by (6) can be written in the following form:

$$\theta_c = 2\arctan\left(\frac{2 \pm \sqrt{4 - r_v^2 + 16\omega_m^2 \tau_L^2 r_v^4}}{r_v - 4\omega_m \tau_L r_v^2}\right). \tag{7}$$

where r_v is as defined in the previous section, i.e, $r_v = V_{\text{ref}}/\hat{V}_{\text{in}}$, and $\tau_L = \frac{L}{R}$. Thus, the bifurcation behaviour is controlled by r_v and τ_L. The two real solutions of (7) (if exist) represent the two critical phase angles θ_{c1} and θ_{c2}. From (7), the condition for existence of these two real solutions in the range of interest $0 < \theta_c < \pi$ is given by

$$\sqrt{\frac{r_v^2 - 4}{16\omega_m^2 r_v^4}} \le \tau_L < \frac{1}{4\omega_m r_v}, \tag{8}$$

which defines the boundaries of the bifurcation regions, as shown in Fig. 8. Furthermore, as θ_{c1} and θ_{c2} get closer

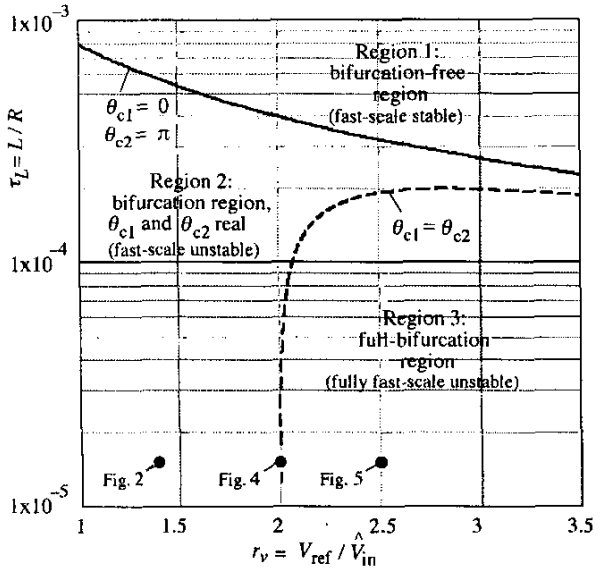

Fig. 8: Instability regions in parameter space. Bullets are parameter values corresponding to waveforms of Figs. 2, 4 and 5.

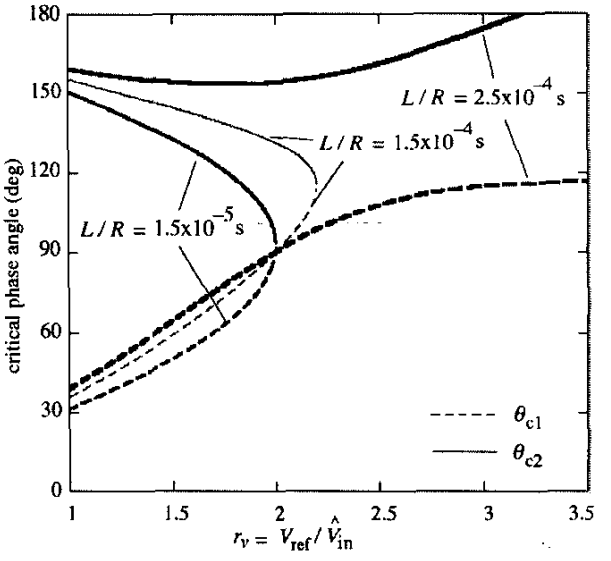

Fig. 9: Critical phase angles versus $V_{\text{ref}}/\hat{V}_{\text{in}}$.

to each other, the stable interval diminishes. If θ_{c1} becomes greater than 90^o, the converter would have gone into period-doubling for the whole first quarter of the line cycle, as we have seen in the simulations.

At the lower boundary $\tau_L = \sqrt{r_v^2 - 4/16\omega_m^2 r_v^4}$ of the bifurcation region defined by (8), we have $\theta_{c1} = \theta_{c2}$, and fast-scale instability cannot be avoided, i.e., period-doubling occurs at some points. Below this boundary, i.e.,

$$\tau_L \leq \sqrt{\frac{r_v^2 - 4}{16\omega_m^2 r_v^4}}, \tag{9}$$

we have the full-bifurcation region where the converter is fast-scale unstable everywhere along the line cycle. This has been confirmed by the simulation result shown earlier in Fig. 5. Moreover, above the upper boundary of (8), i.e., for

$$\tau_L > \frac{1}{4\omega_m r_v}, \tag{10}$$

the solutions given by (7) are essentially outside of the range of interest. In fact, at the boundary $\tau_L = 1/4\omega_m r_v$, we simply have $\theta_{c1} = 0$ and $\theta_{c2} = \pi$, which corresponds to a bifurcation-free or fast-scale stable operation. Finally, in Fig. 9, we plot the critical phase angles given by (7) as a function of r_v, for several values of τ_L. These curves are useful for practical design purposes.

5. CONCLUSION

In this paper we have performed bifurcation analysis to study the effects of various parameters on the stability of the PFC boost converter. It has been shown that this converter exhibits fast-scale instability for certain choices of parameter values. The results obtained here facilitate convenient selection of parameter values to guarantee stable operation.

6. REFERENCES

[1] R. Redl, "Power-factor-correction in single-phase switching-mode power supplies – An overview," *Int. J. Electron.*, **77**(5), pp. 555—582, 1994.

[2] B. Holland, "Modelling, analysis and compensation of the current-mode converter," *Proc. Powercon 11*, pp. I-2-1–I-2-6, 1984.

[3] R. Redl and N.O. Sokal, "Current-mode control, five different types, used with the three basic classes of power converters," *IEEE Power Electron. Spec. Conf. Rec.*, pp. 771–775, 1985.

[4] J.H.B. Deane, "Chaos in a current-mode controlled boost dc/dc converter," *IEEE Trans. Circ. Systs. I*, **39**(8), pp. 680–683, 1992.

[5] W.C.Y. Chan and C.K. Tse, "Study of bifurcations in current-programmed dc/dc boost converters: from quasi-periodicity to period-doubling," *IEEE Trans. Circ. Systs. I*, **44**(12), pp. 1129–1142, 1997.

[6] S. Banerjee and G. Verghese, *Nonlinear Phenomena in Power Electronics: Attractors, Bifurcations, Chaos, and Nonlinear Control*, New York: IEEE Press, 2001.

[7] C.K. Tse and Y.M. Lai, "Control of bifurcation," in *Nonlinear Phenomena in Power Electronics: Attractors, Bifurcations, Chaos, and Nonlinear Control*, Edited by S. Banerjee and G. Verghese, Sec. 8.7, pp. 418–427, New York: IEEE Press, 2000.